Active flow control on a NACA 23012 airfoil model by means of magnetohydrodynamic plasma actuator

P N Kazanskiy, I A Moralev, V A Bityurin and A V Efimov

Joint Institute for High Temperatures of the Russian Academy of Sciences, Izhorskaya 13 Bldg 2, Moscow 125412, Russia

E-mail: fokkoo@yandex.ru

Abstract. The paper is devoted to the study of high speed flow control around the airfoil by means of the Lorentz force. The latter is formed by creating the pulsed arc filament, moving in the magnetic field along the upper airfoil surface. The research was performed for the NACA23012 airfoil model at flow velocities up to 60 m/s (134 mph). The dynamic measurement of the aerodynamic forces on the airfoil was made. Changes up to 5% in an average value of lift and pitching moment were obtained at pulse repetition frequency up to 13 Hz and average discharge power less than 200 W. The amplitude of lift force oscillation was obtained as high as 10%, with the integration time of the balance 30 ms. The dynamic flow visualization of an airfoil model after a single discharge ignition was performed. It is shown that interaction of the main flow with the arc-induced disturbance leads to the dramatic changes in the flow structure. It was shown that the upstream movement of the arc channel (I = 40–700 A) leads to the local flow separation and simultaneously to the formation of a high pressure region above the model surface. Current paper presents investigation of previous work.

1. Introduction

The possibility of significant acceleration of a conducting gas by means of Lorentz force is well-established form the design experience of MHD (magnetohydrodynamic) generators, railguns etc. In plasma aerodynamics the employment of MHD effects was limited by supersonic and hypersonic aerodynamics issues. In [1,2] the discharge was used for acceleration and deceleration hypersonic boundary layer at pressure 28 mmHg and Mach number M = 2.8. In a series of papers [3–13] intensification of mixing was investigated in gas subsonic flow at atmospheric pressure. A great experience was accumulated in investigation of electric arc interaction stirring in a coaxial electrodes configuration.

Different configuration of MHD actuators were used in previous works of aircraft exhaust engine jet noise control [14]. The basic principle of using the MHD acceleration of the arc as a flow control technique is an ability to transfer the momentum from the arc channel towards the surrounding flow. The force-based flow control method can be compared with the fluidic actuators, where the changes in a global flow structure is attained by the blowing of fluid at a particular position of the model. It is known, that the key parameter, determining the efficiency of a fluidic actuator is a jet momentum that should be as high as 0.5% of the pressure head. One should note, that MHD actuators allow creation of the substantial forces, comparable to this value, at least at the lab test conditions. From the other hand, the efficiency of the MHD acceleration is low, leading to the significant heat release in the discharge. The local heat


Content from this work may be used under the terms of the Creative Commons Attribution 3.0 licence. Any further distribution of this work must maintain attribution to the author(s) and the title of the work, journal citation and DOI.
Published under licence by IOP Publishing Ltd

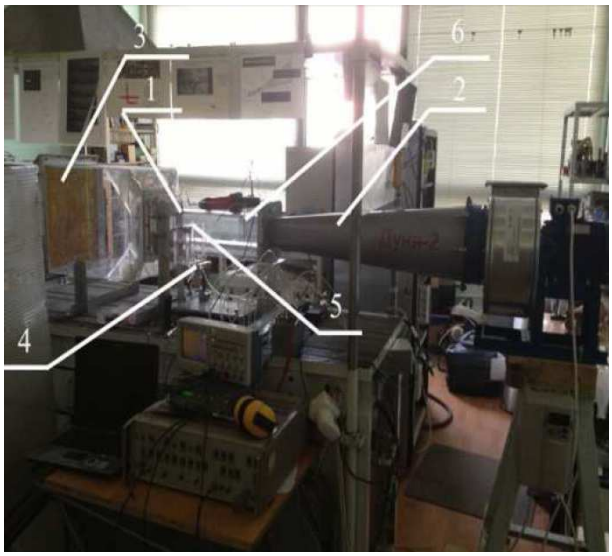

Figure 1. Photo of wind tunnel with of NACA 23012 airfoil model inside. The plasma MHD actuator is switched on. 1—test section, 2—diffuser, 3—honeycomb, 4—strain gauge scales, 5—airfoil model, 6—pitot tube.

deposition density is high enough in comparison with the flow enthalpy, and in its turn, alters the flow structure and should be taken into the analysis. These factors make the MHD-based actuator an interesting object for physical investigation, and, possibly, a perspective candidate for flow control devices.

2. Experimental setup

Tests were cared in the aerodynamic wind tunnel "Dunya-2" with $100 \times 100 \times 300$ test section, operating in a continuous regime. Flow velocity can be changed by controlling the blower motor and was as high as 60 m/s.

The air enters of the wind tunnel was organized from the room of the laboratory through the forechamber. Large-scale flow turbulence was quenched by honeycomb and metal mesh. The airfoil was mounted in the test section on the aerodynamic balance as shown in figure 1. Model was positioned in the test section at a desirable attack angle using rotating mechanisms. Flow blockage was up to 10% at 5° attack angle.

NACA 23012 airfoil model 8 cm × 10 cm (chord × span) was manufactured from ABS plastic by 3D printing method. The part of the upper surface was replaced by a planar ceramic plate, with the discharge organized on its surface. The electrodes were arranged on the surface of the model so than 4 discharge gaps were 34 mm long and 6 mm wide as it can be seen at figure 2. It means that discharge arc covered 24% of the model span. The permanent magnets NdFeB with normal magnetic flux density up to $B = 0.4$ T were mounted under the electrodes. Discharge region was made of ceramics (BK-94) to withstand the temperature in the discharge region.

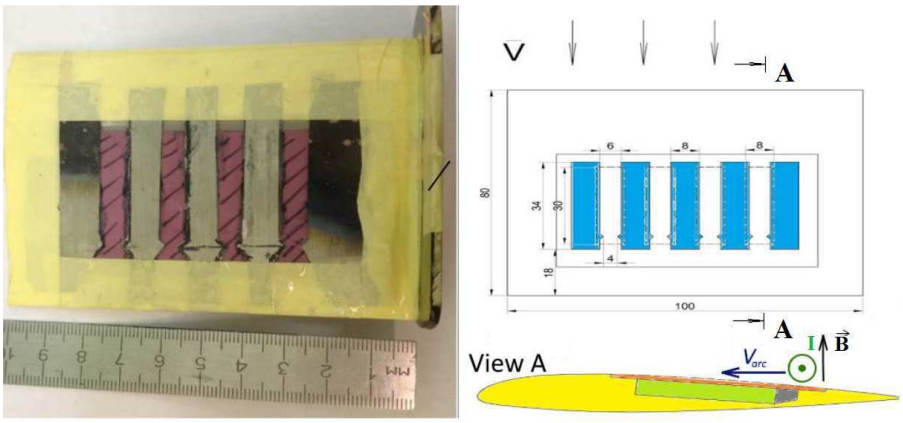

Figure 2. Airfoil model foto on the left, top view and side view A scheme on the right. The electric current I, the velocity vector of the arc V_{arc} and the vector of the magnetic field B are shown.

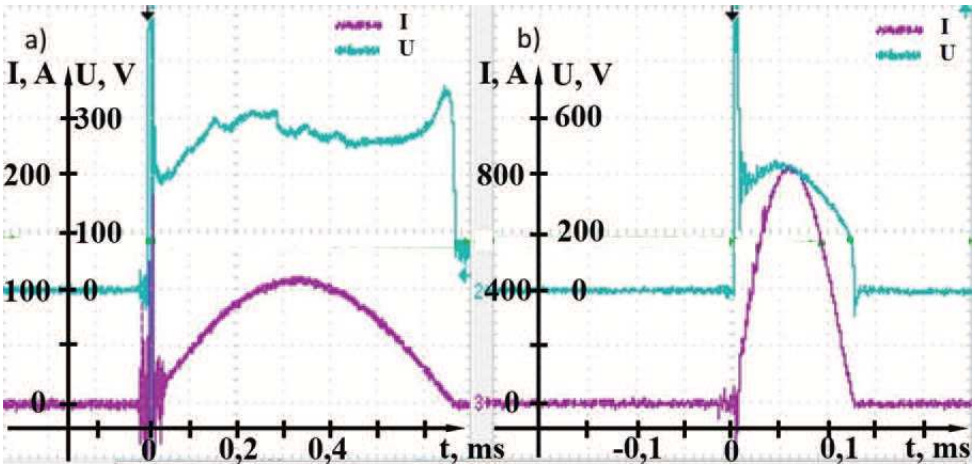

Figure 3. The current and voltage oscillogramms of MHD discharge actuator. (a) Capacitance of the capacitor discharge $C = 10$ μF, inductance of the coil $L = 9$ mH, $I = 70$ A; (b) $C = 10$ μF, inductance of the coil $L = 9$ mH, $I = 700$ A.

The pulsed discharge was created by the pulse generator, based on the LC circuit and a thyratron switch. Pulse amplitude and length were adjusted by altering of the charging voltage and circuit inductance. The typical parameters of pulses were: pulsating current $I < 1$ kA, voltage before discharge ignition $U < 4$ kV, pulse duration $t = 75$–1000 μs, pulse frequency $f_{\text{p}} < 500$ Hz, average power < 1500 W. The current and voltage oscillogramms are shown in figure 3. Breakdown of the discharge was facilitated by barrier discharge between the electrodes and a magnetic underlay.

Discharge voltage was measured with Tektronix P6014A HV (high-voltage) probe, discharge current was measured on 0.1 Ω current shunt. Electrical power input was calculated by digital multiplication of current and voltage signals via TDS 2014B oscilloscope. Flow structure was studied by a LaVision PIV (particle image velocimetry) system, based on 200 mJ NdYAG laser and a 2048×2048 pix camera. Diagnostic equipment was synchronized with the discharge pulses through the frequency divider and delay generator, allowing phase-locked acquisition of data.

Frames were acquired at frame rate ~ 7 Hz, with further averaging of 50–140 images. Accuracy of a single measurement was about 3% (for 40 m/s), while averaging error was several times higher, velocity field resolution was about 1.5 mm. Flow was seeded with TiO_2 particles with the typical size 150 nm and dynamic relaxation time of less than 1 μs.

Aerodynamic balance consisted of 4 tensoresistive sensors (T24A-0.01-C3), dynamic converter (PD-004), and power supply (AIP-012). The limit of force measurement was 10 kg. Accuracy of measurement was $\delta < 0.7\%$. Time resolution was 0.03 s (30 Hz), meaning that any force changes were averaged over this time.

3. Results

The dynamic of the discharge arc in the flow with the magnetic field was studied with high speed camera MotionStudio N. The video was acquired at 30 kHz frame rate with 1 μs exposure along the span of the model. It has been found that the arc velocity at $I = 700$ A and $U = 60$ m/s is up to 150 m/s in the case of co-flow motion and up to 60 m/s in the case of counter-flow motion.

The main results of the aerodynamic force measurements are shown in figure 4. One can see the increase of discharge frequency leads to increase of MHD actuator influence on the flow.

Main change of C_x (drag coefficient), C_y (lift coefficient), M (longitudinal moment) was obtained at maximum $f_{\text{mod}} = 150$ Hz. Higher f_{mod} were unavailable due to the generator power limitations. The largest effect for momentum change was observed when discharge was passing in the counter-flow direction. The largest effect for drag and lift force were observed when discharge was moving in the co-flow direction. The maximum increase of C_x was 1.8% ($V = 60$ m/s) and 5% ($V = 40$ m/s), for C_y 3.1% ($V = 60$ m/s) and 2.3% ($V = 30$ m/s)

It should be noted, that the averaging of these data was held by integration in several seconds after switching on the discharge. Thus, the substantial contribution to measurement results could arise from of thermal deformation of the electrodes and the model. Besides, such algorithm couldn't determine the flow reaction of every single discharge pulse.

PIV visualization of the flow near the airfoil at angle of attack 5° is presented in figure 5. It is possible to trace the evolution of perturbation created by the moving plasma channel in the magnetic field. For all pulse currents major impact of the arc channel on the flow is the formation of shockwave that is followed by the formation of the separation region. The separation point of the flow is following the discharge position. The main steps of the flow evolution can be divided on following processes:

- Electrical breakdown. Weak shock waves are formed at the moment of breakdown. The amplitude of the shock wave decays relatively quickly. The shock wave leads to vortex formation on the sharp trailing edge of the model. It is necessary to mention, that the zone of high pressure is located on the upper side of the wing for more than 0.2 ms and provides significant force effect on the model only during this period of time.
- Major energy input. Major energy input is carried out during 100–1000 μs in studied regimes. The arc channel moves upstream leaving a heated cavern behind. The size of the cavern depends on pulse parameters and arc dynamics during its sweep. The formation of the cavern leads to the external flow change in a manner, similar to the increase of the effective thickness of the profile at the position of the arc.
- Stage of the flow relaxation. After the quenching of the arc channel, the action of the Lorenz force stops and the cavern moves downstream due to the induce pressure distribution. At the same time the thickness of the cavern is getting larger. Relaxation time of the flow is 1.5–2 ms that corresponds to the approximate time passage of the flow along the model chord.

The size of the cavern is affected by main pulse characteristics. Obviously there exist three important values: arc movement speed, gas heating and the arc rise above the surface of the

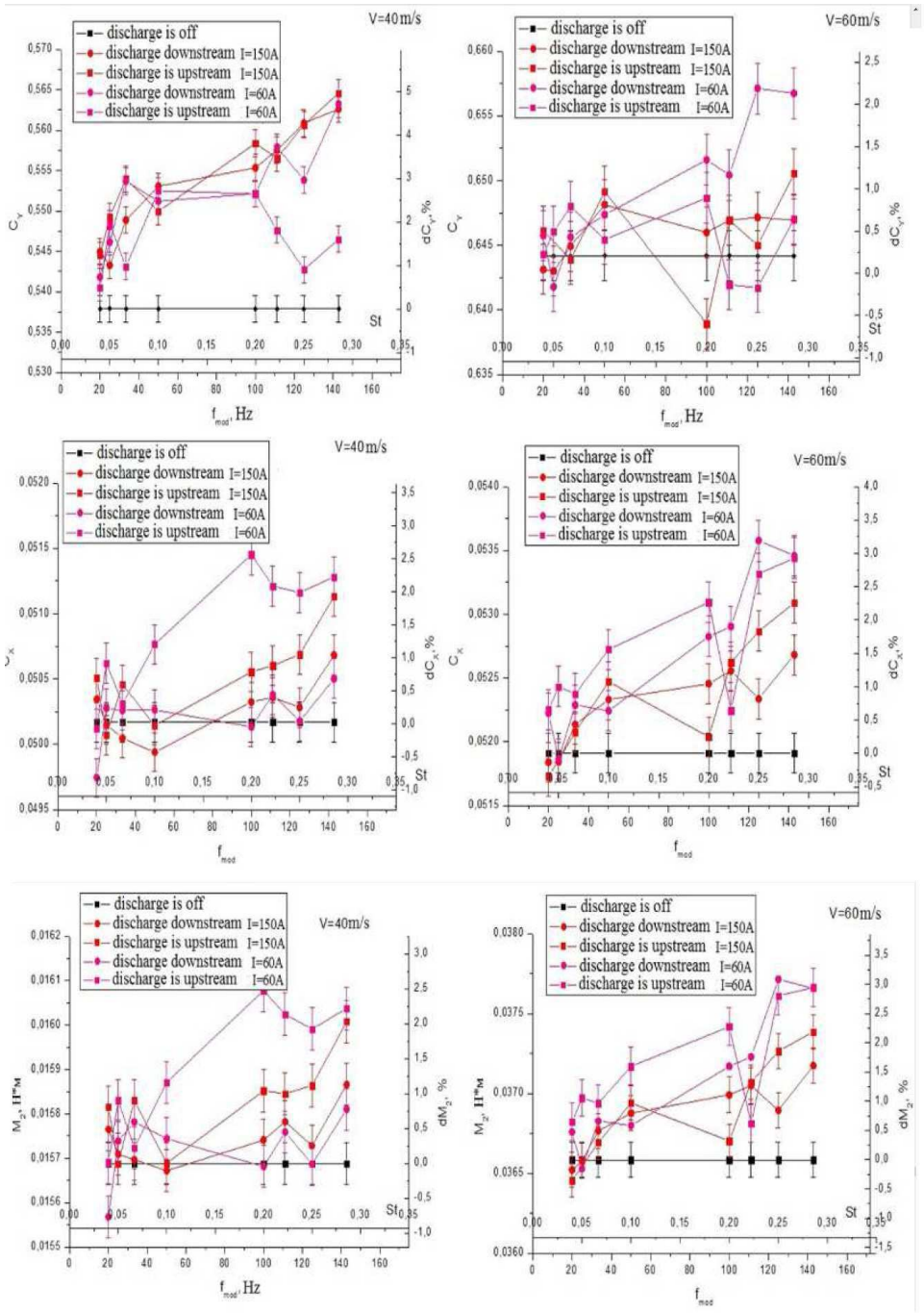

Figure 4. Comparison C_y, C_x and M_z of the airfoil at different modulation frequencies (Strouhal numbers). Left—$V = 40$ m/s; right—$V = 60$ m/s.

model. The length of the perturbation is determined by the distance that discharge makes over the surface of the model. For higher and shorter pulses, short cavern of 15 mm thickness is formed. Size and shape of the cavern are connected to the arc dynamics in the magnetic field at the different values of peak current. At current $I < 100$ A, the field of permanent magnets

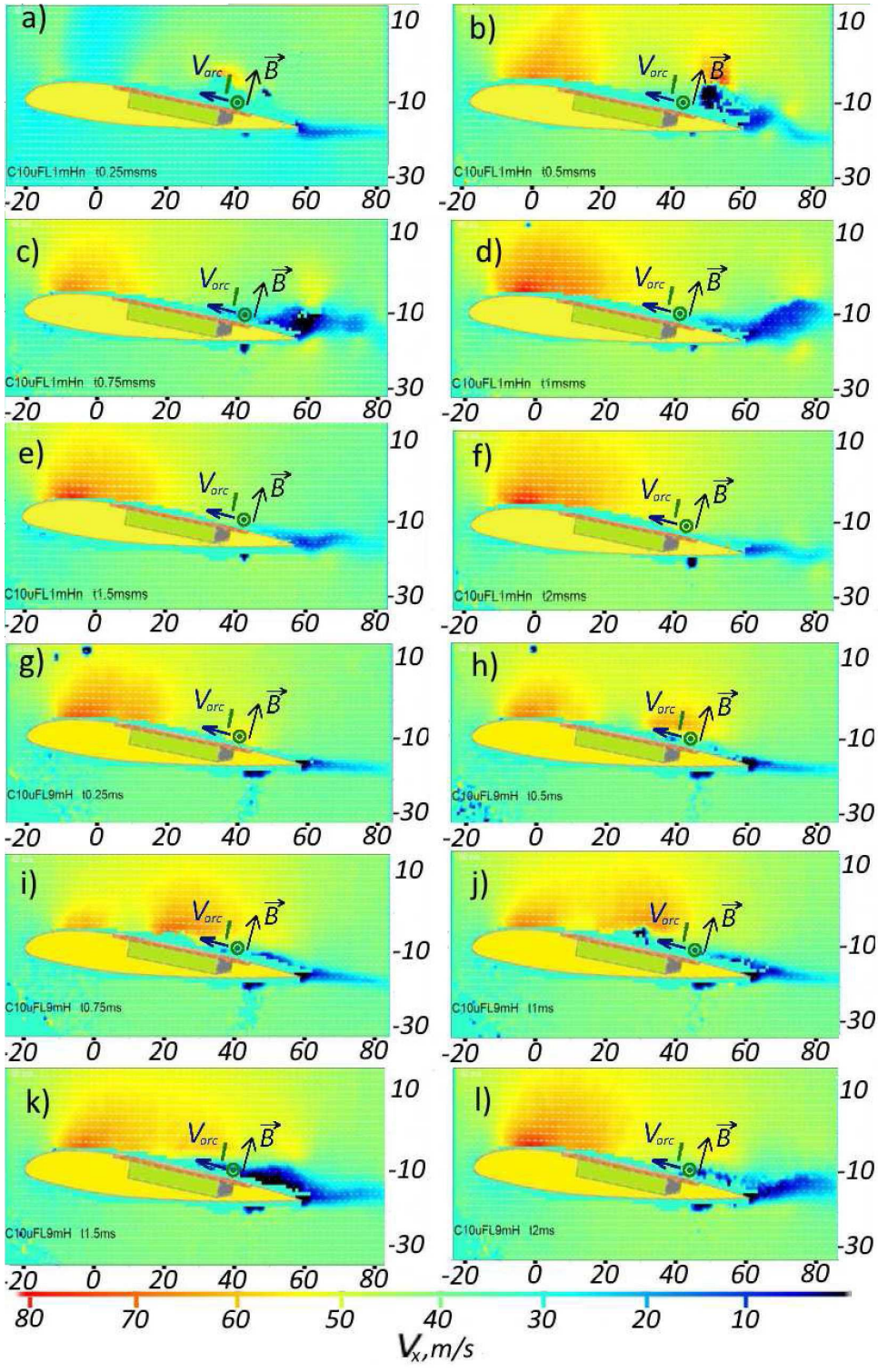

Figure 5. The PIV visualization of the flow near the airfoil at angle of attack 5°. (a)–(f) $I = 700$ A, (g)–(l) $I = 70$ A.

completely determines arc trajectory. Under the discharge current increase, the magnetic field of the arc leads to the increase of the distance between the arc and the model surface. The arc forms a "horseshoe" with the ends situated on the electrodes and the top emerged into the flow. The rise of the discharge under the surface of the model leads to the reduction of the acting Lorenz force that theoretically may lead to the reduction of the effectiveness of the actuator. At the same time the formation of a thicker cavern leads to the higher flowfield perturbation.

The obtained flowfields correlates to the results of the weight measurements. The increase of the lift force, resistance and longitudinal moment observed at the moment of the pulse may be thought to be a result of the flow interaction with the discharge cavern. The forming high speed zones above the cavern after the pulse leads to the pressure decrease at the trailing edge of the profile. Anyhow, the role of pressure increase in the arc during the pulse should be analyzed more accurately.

4. Discussion

The research of plasma actuators flow control around the profile NACA 23012 with unseparated initial flow, at the angle of attack of 5° and flow speed up to 60 m/s was performed.

Flow evolution after a single impulse of MHD actuator, mounded on the downwind side of the profile, has been investigated by PIV. It is shown that the arc speed in the configuration given may come up to 150 m/s. The upward movement of the arc channel with current 40–700 A leads to the formation of the separation region and high pressure in front of the arc and local cavern with reduced pressure behind it. Flow around the cavern and compression wave, spreading under pulse energy input, lead to the short-duration (several milliseconds) increase of lifting force of the model. Therefore, on average the lifting force is growing. The average change of the lift and pitching moment of the airfoil, obtained in the experiment, is 5% under pulse repetition rate of 13 Hz, oscillation amplitude lift up to 10%, moment–up to 5%. It should be noted, the changes in the force, acting upon the airfoil, should take place on the that the timescale of 0.2–5 ms. The balance reaction time did not allow to resolve the high-frequency behavior of the forces, leading to the dramatic (up to 20 times) reduction of the real force amplitude. A comparison of the obtained results with the numerical simulation [15] can be done. The numerical result shows the similar flow structure, with such details as cavern shape and passage time reproducing the PIV results. Anyhow, the detailed comparison of the behavior of lift force shows a significant discrepancy between the numerical and aerodynamic balance results: in the modeling, the discharge pulse leads to the decrease of the force due to the compression region, formed by the arc. This means, that the more detailed analysis of the actuator physics should be done to obtain the full understanding of the actuation mechanism and, consequently, the main scaling parameters of this flow control technology.

5. Conclusion

MHD actuators were tested as an instrument for the flow control on the 80 mm NACA 23012 airfoil at flow velocity up to 60 m/s. It was shown that pulsed actuator operation, mounted within 0.8–0.35% chord, leads to the modulation of force and pitching moment of the airfoil. At flow speed 60 m/s, with the actuator operating at the $I = 700$ A, $F = 13$ Hz the average changes in force coefficients reached $dC_x < 2.8\%$, $dC_y < 6\%$, $dM_z < 7.2\%$, with the amplitude of lifting force and moment reaching 10%. Flow visualization shows that arc movement at the surface of the model in upstream direction leads to the formation of the separation cavern above the model. Cavern forming behind the channel of discharge leads to the pushing off the streamlines from the wall and pressure reduction along the area, covered by cavern.

Acknowledgments

The work was supported by Mil Moscow Helicopter Plant.

References

[1] Zaidi S H, Smith T, Macheret S O and Miles R B 2006 *44th AIAA Aerospace Sciences Meeting and Exhibit* vol AIAA-2006-1006
[2] Macheret S O 2006 *44th AIAA Aerospace Sciences Meeting and Exhibit* vol AIAA-2006-1005
[3] Bityurin V A and Bocharov A N 2001 *39th Aerospace Sciences Meeting and Exhibit Reno, NV, U.S.A* vol AIAA-2001-0793
[4] Bocharov A, Bityurin V, Klement'eva I and Leonov S 2002 *33rd Plasmadynamics and Lasers Conference, Fluid Dynamics and Co-located Conferences* vol AIAA-2002-2228
[5] Bocharov A, Bityurin V, Klement'eva I and Leonov S 2003 *41st Aerospace Sciences Meeting and Exhibit Reno NV* vol AIAA-2003-5878
[6] Bocharov A, Bityurin V, Filimonova E and Klimov A 2004 *42nd Aerospace Sciences Meeting and Exhibit* vol AIAA-2004-1017
[7] Bocharov A, Klement'eva I, Klimov A and Bityurin V 2005 *43 rd Aerospace Sciences Meeting and Exhibit, Reno, NV* vol AIAA-2005-600
[8] Bityurin V, Bocharov A, Klement'eva I, Klimov A and by Institutions F 2006 *44st Aerospace Sciences Meeting and Exhibit, Reno, NV* vol AIAA-2006-1009
[9] Bityurin V, Klementyeva I and Bocharov A 2006 *16th International Conference on Gas Discharges and their Applications* (Xian, China) pp 425–428
[10] Bocharov A, Bityurin V, Klement'eva I and Klimov A 2007 *45th Aerospace Sciences Meeting and Exhibit* (Xian, China: AIAA Pap.) p 1024
[11] Klementyeva I B, Bocharov A and Biturin V A 2007 *Tech. Phys. Lett.* **33** 16–22
[12] Klementyeva I B, Biturin V A, Tolkunov B N and Moralev I A 2011 *High Temp.* **49** 788–796
[13] Pashchina A S, Efimov A V, Chinnov V F and Ageev A G 2016 *Prikl. Fiz.* 29–34
[14] Moralev I A and Zhaketov V D 2012 *The 11th International Workshop on Magneto-plasma Aerodynamics* p 344
[15] Bityurin V A, Boichov C J, Efimov A V, Kazansky P N, Karmatsky R Y and Moralev I A 2014 *The 13th International Workshop on Magneto-plasma Aerodynamics* pp 27–28